CARBON

Electrochemical intercalation of aluminium chloride in graphite in the molten sodium chloroaluminate medium

K.S. Mohandas[a,*], N. Sanil[a], M. Noel[b], P. Rodriguez[c]

[a]*Materials Chemistry Division, Indira Gandhi Centre for Atomic Research, Kalpakkam 603 102, India*
[b]*Central Electrochemical Research Institute, Karaikudi 630 006, India*
[c]*Recruitment and Assessment Centre, Defence Research and Development Organisation, New Delhi 110 005, India*

Abstract

Aluminium chloride intercalation in graphite was studied by anodic oxidation of compacted graphite (rod) and graphite powder electrodes in sodium chloroaluminate melt saturated with sodium chloride at 175 °C. The studies carried out by employing both galvanostatic and cyclic voltammetric techniques had shown that the intercalation reactions take place only beyond the chlorine evolution potential of +2.2 V vs. Al on both the electrodes. The extent of intercalation reaction was directly related to the anodic potential and probably to the amount of chlorine available on the graphite anodes. In the case of graphite powder electrode, a distinctly different redox process was observed at sub-chlorine evolution potentials and this was attributed to the adsorption of chlorine on its high surface area. This finding contradicts a report in the literature that the intercalation reactions occur at potentials below chlorine evolution in the chloroaluminate melt.
© 2002 Elsevier Science Ltd. All rights reserved.

1. Introduction

Metal halide–graphite intercalation compounds have been an important area of investigation in graphite intercalation compounds (GICs). Several metal halides, both oxidizing (e.g. $FeCl_3$, $CuCl_2$) and non-oxidising (e.g. $AlCl_3$, PF_5) were intercalated in graphite by the direct reaction of the metal halide vapour with graphite [1]. Chlorine gas was found necessary for the intercalation of non-oxidising metal halides in graphite and hence it is a deliberate addition in such reactions. Inagaki and Wang developed a new method in which the metal halide intercalation takes place in a molten salt medium [2–6]. In this method, the molten salt mixture contains the metal halide of interest as one of the components. GICs involving $FeCl_3$, $CuCl_2$ and $NiCl_2$ have been prepared this way. There are some reports on the metal halide intercalation by electrochemical method from a molten electrolyte medium [7–9].

As part of our investigations on the electrochemical

behaviour of carbon materials in the molten sodium chloroaluminate medium [10], we have studied the redox processes taking place on two forms of graphite, viz. compacted rod and powder, in NaCl saturated sodium chloroaluminate melt at 175 °C. We have observed that the graphite rod anodes on which chlorine was evolving were disintegrating, whereas the electrodes remain intact below the chlorine evolution potential. Wendt et al. [9] reported a similar behaviour of chlorine-evolving graphite anodes in acidic ($AlCl_3$-rich) sodium chloroaluminate melt at temperatures below 200 °C and attributed this to the formation of aluminium chloride-graphite intercalation compounds in presence of chlorine. Holleck [11] too reported that the graphite electrodes disintegrate in presence of chlorine gas in sodium chloroaluminate melt. Fouletier and Armand [8] reported a study on the aluminium chloride intercalation by anodic oxidation of graphite powders in acidic lithium chloroaluminate melt at 140 °C. In the electrochemical study, the only one of its kind in the literature, the anodic currents observed at potentials below chlorine evolution (+2.1 V vs. Al) were attributed to the oxidation of graphite during intercalation of aluminium chloride. This in other wards means that aluminium chloride intercalation in

*Corresponding author. Fax: +91-4114-280-065.
E-mail address:* ksmd@igcar.ernet.in (K.S. Mohandas).

graphite can take place below the chlorine evolution potential.

In order to resolve the conflicting reports on the intercalation reaction, we have carried out charge–discharge experiments with graphite powder and rod electrodes in basic as well as acidic sodium chloroaluminate melts. We have observed a redox process below the chlorine evolution potential on the graphite powder electrode, whereas it was absent in the case of the compacted rod electrode. The anodic processes were analysed by electrochemical techniques as well as by physical examination of the graphite by SEM and particle size analysis. Our results showed that the anodic process below chlorine evolution potential was related to the surface adsorption of chlorine on the graphite powders whereas the one above chlorine evolution potential on all graphite anodes was due to the oxidative intercalation of aluminium chloride in graphite. The details of the study are reported in this paper.

2. Experimental

Compacted graphite (6 mm diameter rod, 99.9995%, Ultra Carbon, USA) and Graphite powders (average size 6 μm, colloidal graphite, Graphite India, India) were used as electrodes. For cyclic voltammetric experiments, the rod electrodes were embedded in tight Teflon sleeves so that a known area of it (0.5 cm^2) was only exposed to the molten electrolyte in the cell. Approximately 4 cm of the bare electrode was in contact with the melt in the case of the galvanostatic measurements. The graphite powder electrode fabrication was similar to that described in Ref. [12]. Here, 25 mg of the graphite powder with a geometric area of 0.5 cm^2 was used in the cell. All the graphites used were pre-heated under vacuum at 750 °C, for more than 5 h. The bottom surface of the rod electrode was polished thoroughly with 1/0 to 5/0 emery papers and cleaned with ultra-pure acetone.

Sodium chloroaluminate melt was prepared by heating a mixture of vacuum dried sodium chloride (99.9%, Glaxo, India) and sublimed aluminium chloride (99.9%, Fluka, Iron free). The melt was pre-electrolysed with high purity aluminium electrodes (3 mm diameter rod, 99.99%, Leiko, USA) until it looked clear and colourless. Excess NaCl was added to make the melt saturated with NaCl. The purity of the melt was confirmed by cyclic voltammetry on a micro tungsten electrode. The absence of any irregularities between the potential window of the electrolyte (0.0 to +2.2 V vs. Al) was taken as an indication that the electrolyte was free from any impurities.

A pyrex glass vessel with a tight fitting Teflon lid was used as the cell. Aluminium wires (3 mm diameter, 99.99%, Leiko, USA) were used as the counter and reference electrodes. The electrolyte preparation, purification and the experiments as such were performed inside an argon atmosphere glove box, which has purity better than 2
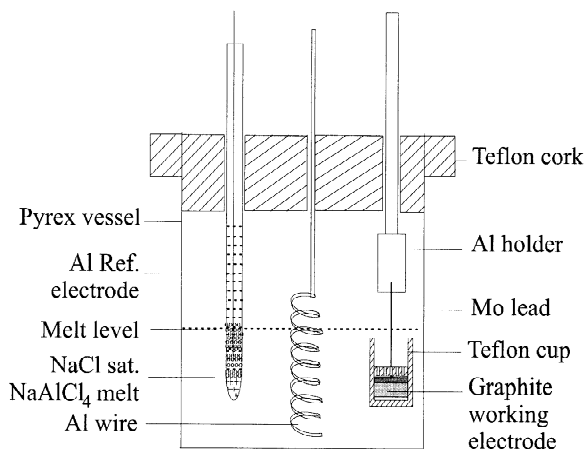

Fig. 1. Schematic of the cyclic voltammetry cell with the graphite powder working electrode.

ppm of oxygen/moisture. A resistance furnace, whose temperature was controlled by a proportional temperature controller (Model IT-401-D2, Indotherm, India), heated the cell. The electrolyte temperature was measured using a chromel–alumel thermocouple. The cell assembly is shown in Fig. 1.

A regulated DC power supply (PGK, Chennai, India) with an accuracy of ±1 mA for current and ±1 mV for voltage was used in the galvanostatic oxidation of the graphite. A constant current discharge unit built in-house with accuracy better than ±0.1 mA and ±0.1 mV was used in the constant current discharge experiments. Cyclic voltammograms were recorded using Potentiostat/Galvanostat (model 173, PAR) coupled to voltage scan generator (EG&G, Universal programmer, model l75). The acquisition and processing of data were carried out with the help of a Data acquisition/switch unit (HP 34970A) interfaced with an IBM compatible computer. A SEM (PHILIPS SEM 501) and a particle size analyser (Malvern Instruments, UK) were used in the surface characterisation of the graphite powders.

The measurements were made generally at 175 °C. The potentials and scan rates of the cyclic voltammetric experiments ranged between +1.0 and +2.5 V (vs. Al in NaCl saturated NaAlCl$_4$ melt) and 1–20 mV s^{-1}, respectively.

3. Results

The galvanostatic charge/discharge curves of the graphite rod and powder electrodes are given in Fig. 2. The anodic currents on both the electrodes stabilise at +2.2 V indicating the chlorine evolution reaction (2Cl$^-$→Cl$_2$+ 2e$^-$). On the graphite powder electrode, in addition to the chlorine evolution, an anodic process starting from +1.4 V
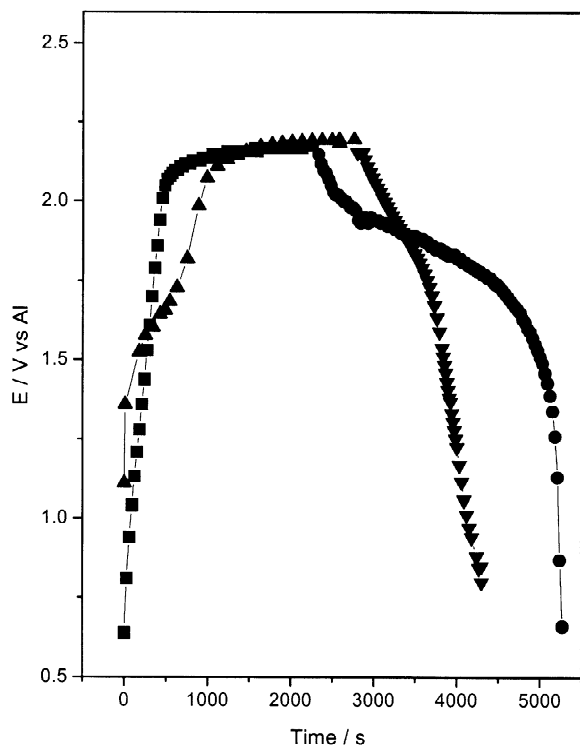
Fig. 2. Galvanostatic charge–discharge curves obtained on graphite rod and powder electrodes at 175 °C. Rod: charge (■), discharge (●) and powder: charge (▲), discharge (▼). The curves obtained with different current densities are combined in the same figure for the purpose of qualitative comparison of the two forms of the graphite electrode.

Fig. 3. Cyclic voltammogrammes obtained on fresh graphite rod (surface area 0.5 cm^2) at 175 °C. Scan rate 20 mV s^{-1}. Five successive cycles with anodic limit increasing from +2.1 to +2.6 V are combined in the figure. The direction of the sweep is shown by the arrows on a typical CV curve. Increase in the magnitude of the cathodic de-intercalation hump with increasing anodic limit shows the direct relationship of anodic potential (chlorine) in the intercalation reaction.

is apparent. On the discharge side, the powder electrode shows cathodic currents extending to far lower potentials than that in the case of the compacted rod electrode.

Typical cyclic voltammmetric curves of a fresh graphite rod electrode with increasing anodic potential limits are presented in Fig. 3. The voltammograms do not show any significant background current or characteristic current peaks in the anodic and cathodic sweeps unless the chlorine evolution potential (+2.2 V) was attained. But when the potential was swept past the chlorine evolution potential, the anodic current increased sharply indicating the evolution of chlorine on the electrode. The corresponding cathodic sweep showed a hump with peak potential ~+1.9 V. As the anodic potential limits were made more and more positive in the successive runs, the cathodic currents also recorded a corresponding increase.

Typical CV response obtained on the graphite powder electrode is given in Fig. 4. A distinctly different feature, as noticed during the galvanostatic polarisation of the powder electrode, can be seen below the chlorine evolution potential. An anodic peak ($i_{p,a}$) and a corresponding cathodic peak ($i_{p,c}$) appear at +1.6 V ($E_{p,a}$) and +1.4 V ($E_{p,c}$), respectively. However, at potentials above chlorine
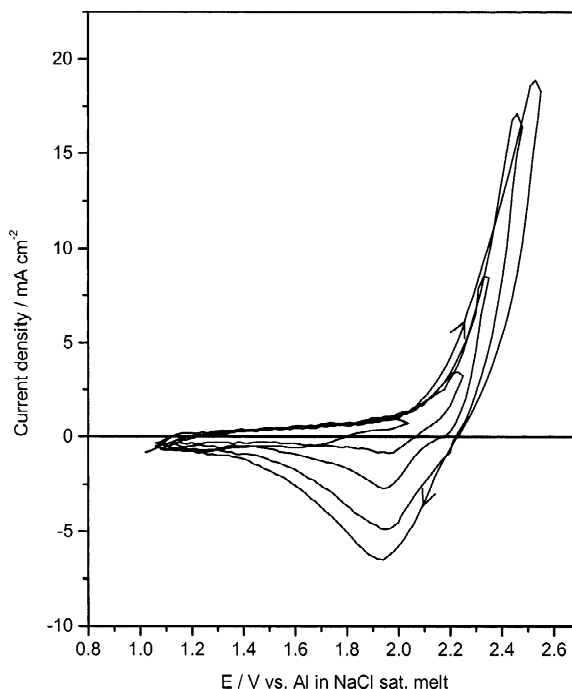
evolution, the electrode behaviour seems to be similar to that of the compacted rod anode. The intercalation and the corresponding de-intercalation processes are evident from the redox peaks in the higher anodic potentials region.

The redox process below chlorine evolution potentials was studied using the CV technique. The CV curves were recorded with different scan rates from 1 to 20 mV s^{-1} and with a fixed anodic potential limit of +1.9 V. The peak separation ($\Delta E_p = E_{p,a} - E_{p,c}$) values of the redox couple were observed to increase with increase in the scan rate (ν), suggesting thereby that it corresponded to a quasi-reversible process. The plots of log ($i_{p,a}$) and log ($i_{p,c}$) against log (ν) show the slopes of the anodic and cathodic processes as 0.74 and 0.84, respectively.

In order to get more information on these redox processes of the powder electrode, CV runs were repeated for about 20 times each on an electrode; first with anodic potential limit below (+1.9 V) and then above (+2.5 V) chlorine evolution. The current values of the successive cyclic voltammograms obtained in the former case were more or less similar whereas those ones obtained in the latter case recorded significant increase with every passing cycle (Fig. 5). The anodic current values of all the cyclic
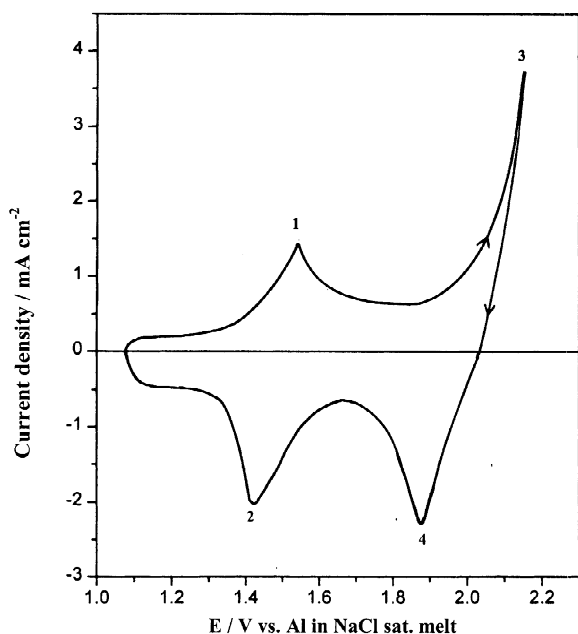
Fig. 4. CV response of the graphite powder electrode at 155 °C. Scan rate 1 mVs^{-1}. The adsorption–desorption (1,2) and intercalation–de-intercalation (3,4) peaks are distinctly seen in the figure.
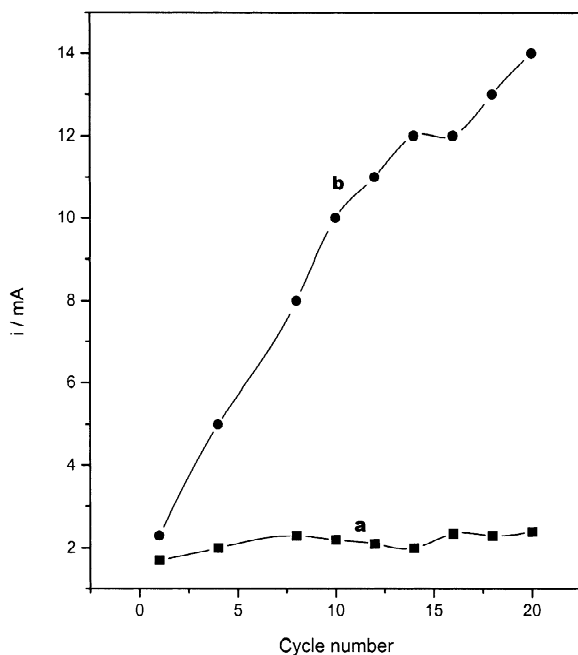

Fig. 5. The effect of the charge–discharge cycling of the graphite powder electrode with and without chlorine evolution on it. Temperature 175 °C. The two curves **a** and **b** are constructed using the anodic currents in the CV at +1.8 V. The anodic potential limits of **a** and **b** were set to +1.9 V (below chlorine evolution) and +2.5 V (above chlorine evolution), respectively.

voltammograms at a uniform potential of +1.8 V were used in the figure for the purpose of comparison. The scanning electron micrographs of the graphite powder before and after the cycling show that the particle size of the graphite powders have increased significantly due to cycling. Particle size analysis of the powders by light scattering method showed that the average size of graphite particles was increased by about ten times (Fig. 6). No significant change in the particle size could be observed in the case of powders cycled with anodic potential limit of +1.9 V, in a separate experiment.

4. Discussion

The results presented above clearly show that both the graphite powder and compacted rod reacted anodically in the melt above the chlorine evolution potential and the reaction products were discharged in the reverse scan to give rise to the cathodic current. The cathodic peak occurs at ∼+1.9 V irrespective of their form. No cathodic currents were observed on the graphite rod electrodes, which were polarised with anodic potential limits below that for chlorine evolution. As graphite does not form stable chlorides with chlorine above 273 K [13], the reversible anodic reaction products can reasonably be confirmed as graphite intercalation compounds (GICs) involving $AlCl_3$ and chlorine, as reported by Wendt et al. [9]. The cathodic process can be considered to be a de-intercalation reaction of these GICs formed during the anodic oxidation above the chlorine evolution potential. A direct relationship between the extent of formation of the intercalation compounds and the anodic potential limit (and the chlorine generated) is evident in Fig. 3. The results clearly show that the aluminium chloride intercalation occurs in molten sodium chloroaluminate only beyond the chlorine evolution potential.

An analysis of the experimental results may indicate that the intercalation reaction is related to the anodic potential as well as the amount of chlorine generated on the electrode. It is known that chlorine is a pre-requisite in the vapour phase intercalation of aluminium chloride in graphite [14,15] and it plays the role of an oxidant for effecting the partial oxidation of graphite necessary for the intercalation reaction. Excess chlorine detected in the GICs also confirmed that chlorine acts as one of the reactants in the vapor phase intercalation reaction. However, chlorine is not expected to play a similar role in the electrochemical intercalation, as graphite gets positively charged by virtue of it being the anode in the cell. So, by hindsight, one would expect the $AlCl_4^-$ ions present in the electrolyte melt to intercalate in the graphite and liberate chlorine when the anodic potential is high enough for the decomposition reaction, $4AlCl_4^- \rightarrow 2Al_2Cl_7^- + Cl_2 + 2e^-$ (+2.6 V). However, the experimental results do not conform to this and
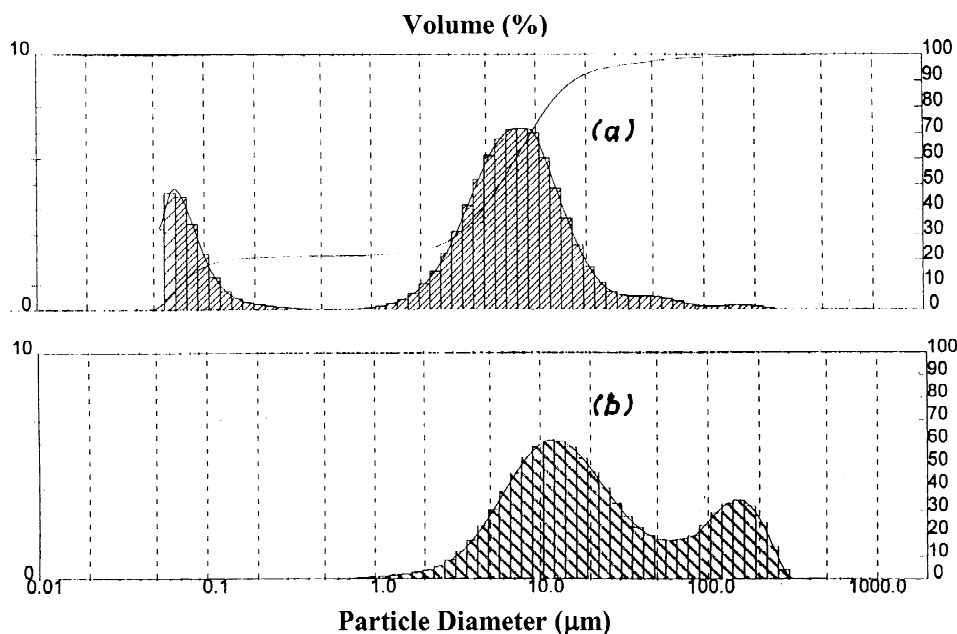
Fig. 6. The particle size distribution of the (a) fresh and (b) cycled graphite powder electrode obtained by light scattering method (Malvern zeta sizer-3). The average size of the powder particles has increased on cycling.

show that the oxidative intercalation takes place at +2.2 V ($2Cl^- \rightarrow Cl_2 + 2e^-$) onwards in the NaCl saturated melt. It may be appropriate to quote here the statement by Wendt et al. [9] that 'at low-temperatures in chloride melts containing free Lewis acid ($AlCl_3$) no chlorine is evolved on graphite because chlorine, together with aluminium chloride, instantaneously form intercalation compounds'. This may suggest that the chlorine is getting consumed in the intercalation reaction. However, owing to the experimental limitations, this could not be ascertained in the present study.

The chlorine stoichiometry for the GICs formed in the vapour phase intercalation of aluminium chloride is known to be around 3.3. This means that for every four $AlCl_3$ molecules intercalated, one excess Cl^- is present in the GIC. Different formulae such as $C_n^+ AlCl_4^- \cdot xAlCl_3$ [16], $C_n^+ Cl^- \cdot 3AlCl_3$ [14] and $C_{18}^+ AlCl_4^- AlCl_3$ [17] have also been proposed. Chemical characterisation of the GICs formed in the present electrochemical intercalation could not be carried out as the excess electrolyte present on the samples interfered with the analysis. Attempts to remove the excess electrolyte destroyed the sample itself. However, from the electrode potentials and the anionic species involved in the reaction, compositions involving C_n^+, Cl^-, $AlCl_4^-$ and $AlCl_3$ can be inferred. Neutral $AlCl_3$ molecules cannot be expected to be present in the NaCl saturated melt, especially at potentials below the decomposition potential of $AlCl_4^-$ ions (+2.6 V). However, under the non-equilibrium conditions existing at the reactive electrode-electrolyte interface, the decomposition of $AlCl_4^-$

ions may become possible at much lower potentials so that free $AlCl_3$ molecules may be present in the GICs.

It is well known that the intercalation reaction is accompanied by swelling of the graphite crystal along the c-axis. During the de-intercalation process, the crystal shrinks with microcracks developing on the surface. The effective surface area of the electrode, therefore, increases substantially with repeated charge–discharge cycles [18]. The increase in the voltammetric currents of the graphite powder electrode, cycled repeatedly with anodic potential limit of +2.5 V (Fig. 5), can hence be reasonably attributed to the increase in the electrode surface area as a result of the intercalation–de-intercalation reaction. The results of the physical examination of the graphite powders also support this (Fig. 6). As intercalation-dependent surface roughening was absent below +2.2 V, the cycling in this potential region does not show any increase in the CV currents.

The preceding discussions suggest that the surface morphological changes observed on repeated cycling of graphite electrodes in the chloroaluminate melt can be taken as the sign of intercalation reaction. When viewed in this context, the absence of any significant changes in the surface morphology or the electrical characteristics of the graphite powder electrode cycled at sub-chlorine evolution potentials suggested that a redox process other than the aluminium chloride intercalation may be occuring in the potential region. The direct relationship of the peak current and the scan rate in the cyclic voltammograms and its further analysis indicate that the redox processes under

question are predominantly adsorption–desorption [19] taking place on the active surface of the fine graphite powder particles. Compared to the compacted graphite material, graphite powder has higher concentration of grain-boundaries, edge-sites and other defects. It is possible that the positively charged graphite powder particles attracts the anionic Cl^- and $AlCl_4^-$ species present in the NaCl saturated melt [20] and the chlorine free radicals adsorb–desorb on such sites to give rise to the redox currents in the sub-chlorine evolution potentials.

$$C_n + Cl^- \Leftrightarrow C_n\text{- - - -}Cl + e^-$$

$$C_n + AlCl_4^- \Leftrightarrow C_n\text{- - - -}Cl + AlCl_3 + e^-$$
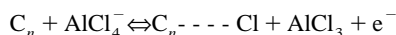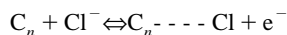
However, Fouletier and Armand [8] considered the anodic currents at $+1.9$ V in the cyclic voltammogram of the graphite powder electrode as one resulting from the aluminium chloride intercalation in graphite. It is mentioned in the paper [8] that the graphite powder particles, under the constant applied potential of $+1.8$ V swelled and at $+1.9$ V exfoliated, characterizing the intercalation reaction. However, no details on the physical examination of the graphite powder are available in the paper.

5. Conclusion

The charge–discharge behaviour of both the graphite rod and powder electrodes in NaCl saturated chloro-aluminate melt at 175 °C shows that the oxidative intercalation of aluminium chloride is possible only beyond the chlorine evolution potential of $+2.2$ V. This finding when read along with the observations made by other researchers on molten chloroaluminate electrolysis with graphite anode suggests that the aluminium chloride intercalation is related to the anodic potential above chlorine evolution and probably to the amount of chlorine generated on the electrode. This aspect of the intercalation reaction, studied by electrochemical means in a molten salt medium, has been reported for the first time in this study. In the vapour phase intercalation of aluminium chloride, chlorine is known to play the role as an oxidant to achieve the partial oxidation of graphite necessary for the intercalation reaction. However, such a role for chlorine in the present electrochemical intercalation reaction seems unlikely. A comparative study of the electrochemical processes on the

two forms of the same graphite material, viz. compacted rod and powder, shows that the anodic process on the latter observed at sub-chlorine evolution potentials is attributable to its physical form and not to the characteristic intercalation reaction. The redox process is identified as the adsorption–desorption of loosely held chlorine free radicals on the active sites of the graphite powder.

References

[1] Zuckerman JJ, Hagen AP, editors, Inorganic reactions and methods, vol 17, New York: VCH Publishers, 1990, pp. 238–42.
[2] Wang ZD, Inagaki M. Synth Metals 1988;25:181–7.
[3] Inagaki M. Synth Metals 1989;34:15–20.
[4] Wang ZD, Inagaki M. J Meter Chem 1992;2:629–32.
[5] Inagaki M, Wang ZD. Synth Metals 1988;20:1–8.
[6] Inagaki M. Carbon 1991;29:423–7.
[7] Inagaki M, Iwashita N, Wang ZD, Maeda Y. Synth Metals 1988;26:41–7.
[8] Fouletier M, Armand M. Carbon 1979;17:427–9.
[9] Wendt H, Khalil A, Padberg CE. J Appl Electrochem 1991;21:929–34.
[10] Mohandas KS. Ph.D thesis, University of Madras 2001.
[11] Holleck GL. J Electrochem Soc 1972;119:1158–61.
[12] Maximovitch S, Levart M, Fouletier M, Nguyen N, Bronoel G. J Power Sources 1978;3:215–25.
[13] Rudorff W. Adv Inorg Chem Radiochem 1959;1:254.
[14] Dzurus ML, Henning GR. J Am Chem Soc 1957;79:1051–4.
[15] Baikar A, Habegger E, Schlogl R. Ber Bunzenges Phys Chem 1985;89:530–8.
[16] Rudorff W, Landel A. Z Anorg All Chem 1958;293:327–32.
[17] Bach B, Ubbelhode AR. Proc R Soc Lond A 1971;325:437–45.
[18] Beck P, Junge H, Krohn H. Electrochem Acta 1981;26:799–809.
[19] Gosser Jr. DK. Cyclic voltammetry—simulation and analysis of reaction mechanisms. New York: VCH Publishers, 1996, p. 43.
[20] Torsi G, Mamantov G. Inorg Chem 1971;10:1900–2.